Novel Approach for Passive Mixing in Microfluidics Utilizing Porous PDMS Sponge

Emil Grigorov
German Engineering Education and Industrial Management
Technical University of Sofia
Sofia, Bulgaria
egrigorov@fdiba.tu-sofia.bg

Boris Kirov
Department Industrial Automation
Technical University of Sofia, 1756
Sofia, Bulgaria
boris kirov@tu-sofia.bg

Jordan A. Denev
Steinbuch Centre for Computing
Karlsruhe Institute of Technology,
Karlsruhe, Germany
jordan.denev@kit.edu

Vassil Galabov
German Engineering Education and Industrial Management
Technical University of Sofia
Sofia, Bulgaria
vtg@tu-sofia.bg

***Abstract*—Mixing in microfluidic devices has been always a significant challenge due to the small channel dimensions and the strongly laminar flow character of the fluids. However, mixing is an essential process in various biological, chemical and pharma processes. This paper introduces a new approach to passive mixing in microfluidic devices, utilizing a quick and cheap way with a sugar cube as prototype to produce a) porous medium. The authors present experimental and numerical analyses of the method, showing that the efficiency of mixing decreases as the volume flow rates of the fluids increase for flows studied with Re in the range 0,028-0,26. The largest porous mediumtested achieved a maximum mixing efficiency of 98%, suggesting that larger geometries may yield even higher efficiencies. A decrease in mixing efficiency along the length of the sponge with increasing volume flow rates was also observed (experimentally and numerically), possibly due to increased backflow. Despite the complexity of the Polydimethylsiloxan (PDMS) sponge, numerical analysis indicates a linear relationship between pressure drop and Reynolds number.**

Keywords - microfluidics, mixing, porosity, PDMS sponge

I. INTRODUCTION

Microfluidics has emerged as a powerful tool for studying biological systems, offering precise control over the operating conditions of the system and enabling a range of applications such as cell sorting, single-cell analysis, and drug discovery. In many microfluidic applications, mixing is required to enable efficient reactions between two or more components. Two or more reactants can be fed through inlet branches and then mixed in a mixing channel. In the discovery and development of new drugs for example, microfluidic devices can be utilized for the rapid screening of a large number of potential drug candidates. Efficient mixing of the drug compounds and biological samples is essential in this case to ensure accurate and reliable results. Due to the low Reynolds numbers (due to the tiny dimensions of the channels) and the strong laminar nature of the flows in microfluidic channels, the process of fluid mixing is strongly diffusion-based and can be therefore relatively slow [1]. For a typical channel width of 200 µm, depending on the diffusion constant of the fluid molecules the penetration distance of a molecule occupying the entire width of the channel may range from 10 to 960 cm [2], which may make cause the construction of channels with unacceptably long lengths.

In the last decades specific methods have been developed to enchage mixing and thus reaction efficiencies in microfluidic devices. Two types of mixing have been already discussed in the literature - active and passive. Based on oscillations in the flow field, active methods utilize external energy sources (e.g., acoustic waves) in order to improve the quality of the mixing reactions [3]. Plenty of existing works show the potential of the implementation of puls induced flows [4] dynamic pressure generators [5] or even active stirring bars [6] in the microchannels. Active mixing methods can be highly effective in achieving rapid mixing; however, the fabrication of active mixers tend to be hard due to the moving parts and the need of an external power source [7]. Passive mixing, on the other hand, is achieved by changing the configuration of the microchannels during the fabrication stage. This approach often involves the use of geometrical features, (e.g., obstacles or spirals) in order to accelerate the diffusion between the two fluids through fluid stretching, folding or breakup. In other words, an essential condition for good mixing is the ‘crossing’ of streamlines [7]. As described in their work [8] this process, in which the fluid undergoes a series of chaotic and unpredictable motions that enhance mixing by disrupting the fluid layers and promoting the molecular exchange between different regions can be roughly equated with “chaotic advection”. A variety of novel geometrical design and concepts of micromixers based on this principle have been investigated in the last several years, several of which will be presented briefly here.

In their work Chung et al. [9] presented a variation of the traditional T-mixer, utilizing a rhombic micromixer with flat angles. The results showed that a mixing efficiency of more than 93% could be achieved at Reynolds numbers greater than 180 due to the development of a recirculation effect around the structures. Similarly, Li et al. [10] proposed a mixer with improved geometry, which with the help of sub-channels „splits and recombines“ the fluids streamlines. The experimental and numerical results showed mixing performance between 70% and 86% for Reynolds numbers in the range 1-80. Yang et al. [11] utilized a three-dimensional spiral micromixer consisting of two overlapping channels in order to induce a chaotic mixing effect. It was experimentally shown that a mixing efficiency of 90% could be reached by adjusting the flow rates and the geometries of the channels. Similar mixing efficiencies were observed in the three-

dimensional chaotic micromixer of Li et al. [12], consisting of periodic triangular mixing chambers. The results were confirmed by several numerical simulations.

This paper presents a new approach to achieve passive mixing within a microfluidic device through the integration of a porous medium. Previous studies, not specifically related to microfluidic flows, including those conducted by [13] and [14], have extensively examined mixing mechanisms within porous media. It has been demonstrated that enhanced mixing efficiency is achieved through the interaction between local velocity fluctuations and diffusion. Mixing within porous media occurs as a result of stirring fluid elements and the creation of lamellar structures [13]. This brings initially segregated solutes into close proximity, allowing them to homogenize through diffusion. Additionally, the spreading of the solute distribution through advective stirring also accelerates the mixing process.

The porosity in our microfluidic device was created using the matrix of a simple sugar cube. The mixing efficiency was evaluated using captured microscopic images and an image processing technique for various inlet velocities of the two fluids to be mixed. Furthermore, one of the device's geometries was analyzed numerically.

II. Methods and Chip Fabrication

The microfluidic device's geometry was initially designed using computer-aided design (CAD) software. The model's mold was subsequently produced using an LCD-based stereolithographic 3D printer (Phrozen Sonic Mini 4K). A premixed polydimethylsiloxane (PDMS) pre-polymer was then poured into the printed master, and cured in an oven at 60 ◦C for 1 hour. After removing the hardened chip from the resin, a proportionate PDMS sponge, was placed inside the mixing chamber. The chip and a microscope cover slip were exposed to oxygen plasma treatment and subsequently fused together.

TABLE I Dimensions of the investigated mixing chambers

Geometry	W x H [mm]
1	2x2
2	3x3
3	4x4

The model consists of two inlet channels and one exit channel, each having the dimensions 200 x 200 µm, as shown on Fig. 1. The mixing chamber has the length of a standard sugar cube – 11 mm, however the width and the height of the chamber were varied according Table I, in order to investigate the dependency of the mixing efficiencies form dimensions of the chosen sponge.

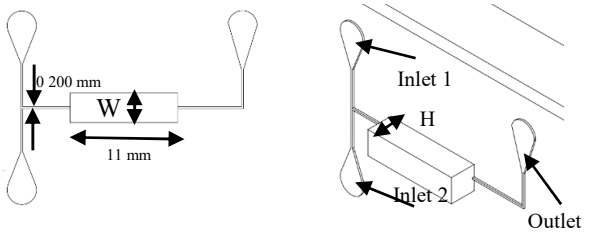

a)

b)

Fig 1 A schematic of the geometry and the dimensions of the utilized model in a) and the real chip with the integrated PDMS sponge in b).

The methodology for the fabrication of the PDMS sponge has been extensively documented in [15]. The process involves placing a sugar cube in a Petri dish that contains a mixture of the PDMS pre-polymer, as specified in the previous section. Subsequently, the sugar cube infiltrated with the polymer mixture is subjected to a temperature of 60°C for 2 hours in an oven to ensure complete PDMS polymerization. Once the polymerization process is complete, the composite is transferred to a freezer for a duration of 3 minutes to facilitate detachment of the PDMS from the polymer. Finally, the sugar crystals are removed by rinsing with deionized water at a temperature of 60°C for a duration of 1 hour. Fig. 2 shows the sugar cube and the resulting squeezed PDMS sponge.

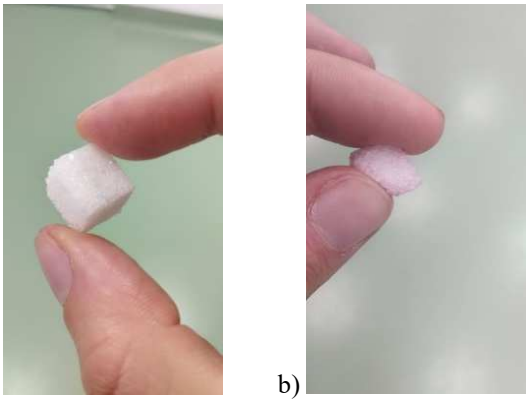

a) b)

Fig. 2 In a) the utilized sugar cube, in b) the resulting squeezed PDMS-sponge

According to the work of [15], in which a micro-computed tomography (µCT) on the PDMS foam was conducted, the porous PDMS sponge has complex interconnected pore channels with a widely polydisperse volume along the different its matrix. The analysis showed that the porous structure had a smooth internal surface area with a macro-pore size in the range of 500 ± 300 µm and a porosity of about 77%. In the present work the same procedure for the production of the porous media is kept and therefore the given size of the pores is assumed to be identical.

To conduct the experiments, in the present work two syringe pumps were employed to deliver the fluids. The experiments were visualized using an in-house 3D-printed, inverted microscope with a picture resolution of 640 x 480. Distilled water (DW) and DW + azorubine red dye, were used as the two fluids for the mixing experiments.

A. Evaluating Mixing Efficiency

To quantify the efficiencies of mixing in the experimental setup, we performed image processing on the microscopic images captured at the exit of the mixing chamber. This involved using a python-based software tool that enabled the

user to draw a line across the cross-section of the image. The selected area was then converted into a gray-scale format. The evaluation of the mixing efficiency was carried out by analyzing the dispersion of pixel intensities along this grayscale line. Fig. 3 illustrates the process steps using the example of an area where no mixing was observed, i.e., prior to the two fluids entering the porous sponge.

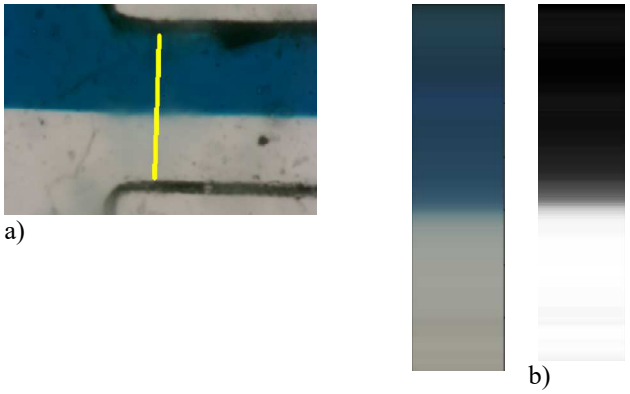

a) b)

Fig. 3 In a) the microscope image with the drawn line. In b) up the colors of the section marked by the line and the corresponding grayscale distribution.

Fig. 3 a) displays the colors of the selected line, while Fig. 3 b) shows the corresponding grayscale image. The deviation of the average gray intensity around the gray pixel, corresponding to the mixed region in the middle of the channel, was computed for the pixels of the selected line using (1):

$$\sigma = \frac{\sqrt{\frac{1}{N}\sum_{i=1}^{N}(\bar{G} - G_i)^2}}{\bar{G}} \qquad (1a)$$

, where σ is the standard deviation of the pixel intensities along, $\bar{G}$ denotes the average grey intensity and G_i represents the actual grey intensity of the i-th pixel along the line. The standard deviation is equal to 1 when there is no mixing, whereas at full mixing, it will reach 0, as all the pixels attain a uniform grey intensity. This approach has been previously demonstrated in the work of [16]. The actual mixing efficiency in percentage is then calculated according (2):

$$M_{eff} = (1 - \sigma) \cdot 100\% \qquad (2)$$

B. Numerical Simulation

The proposed method for evaluating the mixing efficiency has a drawback, namely that it is based solely on a single plane defined by the microscope image, whereas the mixing process, as described in the introduction, is typically driven by three-dimensional effects. To address this limitation, a numerical simulation was performed. Building on the work of [15], which included a µ-CT analysis that successfully captured a video of the PDMS foam structure, a three-dimensional geometric model of the sponge was developed. A python-based script was utilized to split the aforementioned video into separate frames, and an open-source software tool (Seg3D2), which is typically used in medical imaging applications for volume segmentation and processing, was employed for image processing. As shown in Fig.4 the porosity was successfully reconstructed. However, due to the highly complex faces and geometries involved, the creation of the model was computationally demanding in terms of memory and CPU usage, and therefore, only geometries 1 and 2 from Table 1 were reconstructed.

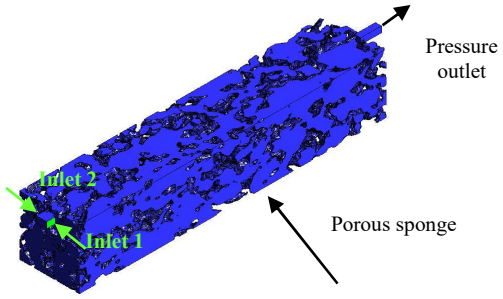

Fig 4. The constructed 3D model of the PDMS sponge on example of Geometry 2 from Table 1

For the simulation and discretization of the 3D model an Ansys Fluent 21R2 with the implemented species transport model [17] was utilized to solve the system of partial differential equations described below (3-5). The utilized discretization grid consists of around 26,2 million tetrahedral elements. The boundary conditions consist of constant velocity profile for the two inlets, a pressure outlet with p = 0 Pa at the exit channel after the mixing chamber, and no-slip boundary conditions for the walls. The computations are carried out as steady-state. All parallel computations had a wall-clock-time of 30min, before desired residual criteria of $1x10^{-4}$ for the continuity, velocity components, pressures and species concentration were reached. For all described simulations 160 cores on the "bwUniCluster 2.0" at Karlsruhe Institute of Technology were utilized.

The equations utilized for the discretization of the problem are shown below. Eq. (3) represents the mass conservation (continuity) equation for incompressible fluids, whereas Eq. (4) is the momentum transport equation:

$$\rho\nabla \cdot (\mathbf{U}) = 0 \qquad (3)$$

$$\nabla.(\rho\mathbf{U}\mathbf{U}) = -\nabla p + \nabla \cdot (\mu[\nabla\mathbf{U} + \nabla\mathbf{U}^T]) \qquad (4)$$

The density ρ and the viscosity µ were for both fluids were chosen to be 1 x 10^3 kg/m^3 and 1 x 10^{-3} Pa s respectively. U is the velocity vector (m/s) and p the pressure (Pa). When modelling mixing problems, one should always include the diffusion of the species in the fluids. This transfer is taken into account in the form of a convection-diffusion equation (5), as shown below:

$$\mathbf{U} \cdot \nabla c = \nabla \cdot (D\nabla c) \quad , \qquad (5)$$

where c represents the concentration of the species (mol/m^3) and D the diffusion coefficient (m^2/s). Since the concentration of the utilized red dye between the working fluids is negligibly small compared to the fluid volumes, self-diffusion of pure water was used for the simulations. The diffusion coefficient for water molecules in water was taken from [18] at D = 2.29 µm2/ms.

Table 2 summarizes the utilized boundary conditions for the simulated geometry. For every simulation both fluids had equal inlet velocities. The listed values in column 2 correspond to the volume flow rates utilized in the experimental part - 0.2 ml/h, 0.6 ml/h, 0.9 ml/h, 1.2 ml/h, and 1.9 ml/h, the results from which will be presented in the result section. The corresponding Reynolds number (Re = ρ·L·u/µ,

with L equal to the width of the channel 200µm), is also presented in Table 2.

TABLE II Inlet velocities and Re numbers.

Case	Channel Inlet velocity [m/s]	Re
1	0,00139	0,02778
2	0,00417	0,08333
3	0,00625	0,12510
4	0,00833	0,16667
5	0,01319	0,26389

Similarly, to (2), the mixing efficiency for the above-presented numerical simulations, was evaluated according (6), also utilized in [19]:

$$M_{eff} = 1 - \frac{\sqrt{\frac{1}{N}\sum_{i=1}^{N}(\bar{c}-c_i)^2}}{\bar{c}} \quad (6)$$

where c_i and $\bar{c}$ represent the mass fraction of the fluid in the i-th mesh control element and the average mass fraction of the fluid on the whole cross-sectional area of the outflow.

In the first part of the result section the experimental findings concerning the three geometries from Table 1 are discussed. Fig. 5 presents the mixing efficiencies evaluated in the channel immediately downstream the PDMS sponge, as a function of the Reynolds number (Re). Every point represents the average over two separate experiments in a different microfluidic chip.

From the data, we can observe that for all three geometries, there is a decrease in the mixing efficiency index as the Reynolds number (inlet velocities) increases. This can be explained by the fact that as the flow rate increases, the residence time of the fluids within the pores of the sponge decreases. This reduced residence time means that there is less time for the diffusive-dominant process of mixing to occur, leading to a lower mixing efficiency index.

This observation is consistent with previous research [14], which has shown that a central issue for mixing in porous media is the fact that characteristic diffusion times may be several magnitudes larger than characteristic advection times. In other words, while the flow may spread or stir the fluids within the sponge, it may not be sufficient to mix them effectively. This could also explain the slopes seen in Figure 5, where we observe a decrease in mixing efficiency index as the Reynolds number increases.

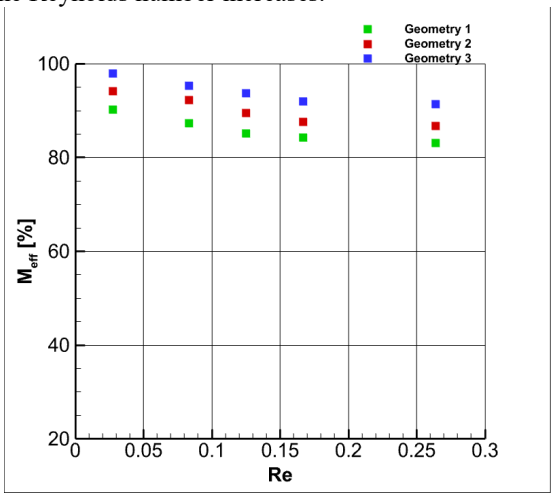

Fig. 5 Mixing efficiency of the conducted experiments as a function of the Re number for the three geometries described in Table 1.

Fig. 5 shows a clear improvement in mixing efficiency with increased sponge dimensions. On average, a 6-7% increase in mixing efficiency can be observed for a fixed Reynolds number when the sponge size is increased. This improvement can be largely attributed to the fact that larger sponges provide more homogeneous spreading and distribution of the fluid across the cross-section of the geometry, as well as longer residence times and contact between the two fluids inside the channels of the foam. These factors lead to a more uniform mixing process with fewer pockets of unmixed fluids. The maximum achieved mixing efficiency was 97.8% for the lowest Reynolds number and the largest sponge size of 4mm x 4mm, while the lowest efficiency index was found to be equal to 82.1%.

When comparing the results obtained from numerical simulations to the experimental mixing efficiency, as shown in Fig. 6 for Geometry 1 in Table 1, there is a difference in the slopes of development. The results were calculated on the cross-section of the exit channel (the channel just after the sponge exit - Fig. 4). At low Reynolds number values, the simulation results exceed the experimentally obtained mixing values by 8%. For high Reynolds number values, the numerical values become lower than the experimental mixing values by less than 5%. Even though these differences are relatively small and the data between experiment and simulation are is a good agreement, there are to several factors, which can explain them. Firstly, the simulated geometry does not perfectly correspond to the porous sponges used in the experimental study. In order to obtain a closer numerical description of the mixing in the porous medium of the PDMS sponge, numerous other models, based on different sugar cubes have to developed. Additionally, even though a high-quality mesh was utilized for the CFD simulation, there is still numerical diffusion present, which can lead to a non-physical increase in the efficiency of the numerical results. Furthermore, the different areas utilized for calculating mixing efficiency (line for the experimental pictures and area for the numerical simulations) could be the reasons for the different slopes for the numerical and experimental results from Fig. 6.

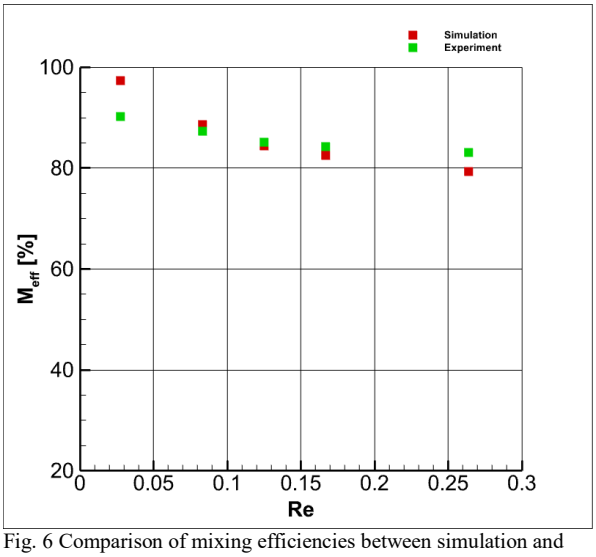

Fig. 6 Comparison of mixing efficiencies between simulation and experiment for Geometry 1 in Table 1.

Further analysis of the mechanisms driving mixing in the presented PDMS sponge can shed light on the local development of the mixing index. Fig. 7 displays the effective mixing index (M_{eff}) as a function of the length of the PDMS

sponge for the numerically investigated Reynolds (Re) numbers. The results reveal that the mixing efficiency between the two fluids is enhanced not only at the exit of the geometry, but also along the length of the sponge, particularly for the higher Re numbers. An interesting phenomenon that emerges is the observation that, for the highest volume flow rates, a slight decrease in the mixing percentage can be discerned between the 5th and 7th mm of the foam. This decrease can be attributed to the negative velocities in the axial direction within the PDMS foam, which arise from the structure of the geometry and cause backflows. Another interesting observation is the difference of around 10% in the mixing efficiency at the first mm for the various volume flow rates. This difference can be ascribed to the longer residence time of the fluids for lower Re numbers, and is most pronounced at the entry of the PDMS sponge, where the fluid exits the channel with smaller dimensions.

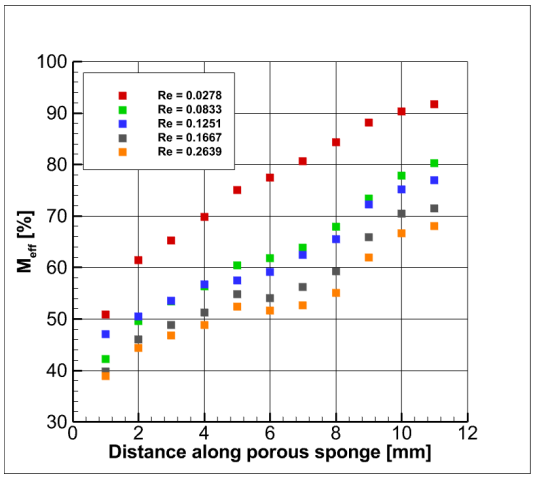

Fig. 7 Numerical mixing efficiency along the length of the PDMS sponge for the simulated Re numbers

The analysis of pressure drop across porous media is critical in the study of fluid dynamics, particularly in microfluidics, where large pressure drops can impede fluid progression through the medium, leading to incomplete mixing, reduced efficiency, and potential chip leakage. Fig. 8 displays the pressure differential ($\Delta p = p_{in} - p_{out}$) between the entry and exit points of the foam, emphasizing the importance of pressure drop in such systems. Through data analysis, it is evident that pressure drop increases linearly with Reynolds number, a behavior typical of the laminar flow regime [3].

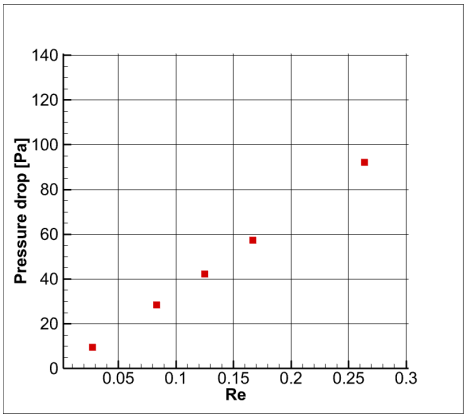

Fig 8. Pressure drops of Geometry 1 from Table 1 as a function of the Re number

III. Conclusion

The present paper describes a novel passive mixing method, based on the integration of a porous medium in a microfluidic device. This paper presents a novel approach for passive mixing in microfluidic devices, which involves the use of a porous medium. To the best of the authors' knowledge, this is the first time that a porous medium has been implemented for mixing within a microfluidic device.

Both experimental and numerical analyses revealed that the efficiency of mixing decreases as the volume flow rates of the two fluids increase in the range Re = 0.028-0.26, similar to the results shown in [20]. The largest sponge tested (4 mm x 4 mm) achieved a maximum mixing efficiency of 98%, suggesting that even greater efficiencies may be possible with larger geometries. Moreover, it was observed that the efficiency of mixing decreased along the length of the foam as the volume flow rates increased. This may be due to the backflow increasing inside the geometry, although further investigation is required to confirm this. Despite the complex structure of the polydimethylsiloxane (PDMS) sponge, as reported in previous studies [15], the numerical analysis indicated a linear relationship between the pressure drop across the geometry and the Reynolds number, consistent with existing literature.

One of the intended purposes of our device is the cleaning and separation of biological samples containing complex fluid mixtures (i.e. stomach liquid, etc.). In fact, we plan the application of the mixer as a DNA extractor from rumen extracted from living sheep in a project dedicated to ruminant rumen microbiome optimization for reduced methane emissions.

Acknowledgment

The experimental and theoretical work described here was partially funded by bulgarian national grant KP-06-N56 / 4. We also acknowledge the comprehensive support of RDIC and Sofia Tech Park. The authors appreciate the CPU-time on the supercomputer “bwUniCluster 2.0” at the Steinbuch Centre for Computing of the Karlsruhe Institute of Technology granted by the project “bwHPC-S5” of the Ministry of Science, Research and the Arts of Baden-Württemberg, Germany.

References

[1] K. Ward and Z. Fan “Mixing in microfluidic devices and enhancement methods” in Micromech. Microeng, vol. 25, 2015, 094001J

[2] J. Ottino and S.Wiggins, “Introduction: mixing in microfluidics” in Phil. Trans. R. Soc. Lond. AJulio, 2004, 923-935

[3] CC. Chang, LM..Fu and RJ. Yang, “Active Mixer” In: Li, D. (eds) Encyclopedia of Microfluidics and Nanofluidics. Springer, Boston, MA, 2008, p.33-38

[4] I. Yasumasa and K. Satoru. “A vibration technique for promoting liquid mixing and reaction in a microchannel.” in AIChE Journal. Vol. 52., 2006, p.3011 - 3017.

[5] C. Chen, P. Li, T. Guo, S. Chen, D. Xu, and H. Chen, “Generation of Dynamic Concentration Profile Using A Microfluidic Device Integrating Pneumatic Microvalves” in Biosensors, vol. 12, 2022, 868.

[6] PY.Gires, M. Thampi, and M. Weiss, “Miniaturized magnetic stir bars for controlled agitation of aqueous microdroplets” in Sci Rep 10, 2020, 10911.

[7] C. Campbell, and B. Grzybowski, Bartosz. “Microfluidic mixers: From microfabricated to self-assembling devices” in Philosophical

transactions. Series A, Mathematical, physical, and engineering sciences. Vol. 362. 2004, 1069-86.

[8] S. Wiggins, JM. Ottino "Foundations of chaotic mixing" in Philos Trans A Math Phys Eng Sci. vol. 15, 2004, p.937-70.

[9] C. Yung-Chiang, H. Yuh, J. Chung, L. Ming, L. Yu "Design of passive mixers utilizing microfluidic self-circulation in the mixing chamber" in Lab Chip, vol. 70, 2004, 1473-0197

[10] J. Li, G. Xia and Y. Li "Numerical and experimental analyses of planar asymmetric split-and-recombine micromixer with dislocation sub-channels" in J. Chem. Technol. Biotechnol., 88, 2013, pp. 1757-1765

[11] Y. Yang, L. Qi, Y. Chen and H. Ma "Design and fabrication of a three dimensional spiral micromixer" in Chin. J. Chem., 31 2013, pp. 209-214

[12] L. Li, Q. Chen and C.T. Tsai "Three dimensional triangle chaotic micromixer" in Adv. Mater. Res., 875–877, 2014, pp. 1189-1193

[13] E. Villermaux, "Mixing by porous media" in Comptes Rendus Mécanique, Vol. 340, Issues 11–12, 2012, p. 933-943

[14] P. Anna, J. Jimenez-Martinez, H. Tabuteau, R. Turuban, T. Borgne, M. Derrien, and Y. Méheust "Mixing and Reaction Kinetics in Porous Media: An Experimental Pore Scale Quantification" in Environ. Sci. Technol., vol. 48, 2014, 508–516

[15] J. González-Rivera, R. Iglio, G. Barillaro, C. Duce, M.R. Tinè, "Structural and Thermoanalytical Characterization of 3D Porous PDMS Foam Materials: The Effect of Impurities Derived from a Sugar Templating Process" in Polymers, vol. 10 2018, 616

[16] Yakhshi-Tafti, Ehsan, H. Cho and R. Kumar, "Diffusive mixing through velocity profile variation in microchannels" in Experiments in Fluids. Vol 50. 2010, 535-545.

[17] I. S. Jacobs and C. P. Bean, "Fine particles, thin films and exchange anisotropy," in Magnetism, vol. III, G. T. Rado and H. Suhl, Eds. New York: Academic, 1963, pp. 271–350.

[18] R. Mills "Self-diffusion in normal and heavy water in the range 1–45◦". J. Phys. Chem. 1973, 77, 685–688.

[19] E. Nady, G.Nagy, R. Huszánk and R. Nicole "Improvement in mixing efficiency of microfluidic passive mixers functionalized by microstructures created with proton beam lithography" in, Chemical Engineering Science, Vol. 247, 2022, 117006,

[20] W. Raza, S. Hossain, K. Kim, " A Review of Passive Micromixers with a Comparative Analysis". Micromachines 2020, 11, 455.